International Journal of Advances in Engineering and Management (IJAEM)
Volume 6, Issue 09 Sep. 2024, pp: 499-508 www.ijaem.net ISSN: 2395-5252

Effect of Nanoparticle Concentration on Thermophysical Properties and Heat Transfer Performance of Aluminum Oxide ($Al_2 O_3$) Nano-lubricants in a Cylindrical Channel: A Numerical Investigation

[1]Itabiyi, O. E., [2]Sangotayo, E.O*., [3]Akinrinade, N.A and [4]Muraina, A. B.

[1,2]*Department of Mechanical Engineering, Ladoke Akintola University of Technology, Ogbomoso, Nigeria,*
[3]*Department of Mechanical Engineering, Bells University of Technology, Ota, Ogun State, Nigeria,*
[4]*Department of Work and Maintenance, Bells University of Technology, Ota, Ogun State, Nigeria,*

Date of Submission: 15-09-2024 Date of Acceptance: 25-09-2024

ABSTRACT:
This study examined the effect of nanoparticle concentration on the thermophysical properties and heat transmission characteristics of nano-lubricants made from aluminum oxide ($Al_2 O_3$) in a cylindrical channel. Nano-lubricants, which are made by dispersing nanoparticles into base fluids, have gained popularity for their ability to improve heat transfer performance. The numerical investigation includes altering the nanoparticle size ($0.0<\varphi<0.5$) of the $Al_2 O_3$ -based nano-lubricant and determining critical parameters such as thermal conductivity, viscosity, specific heat, and heat behavior in the channel. The governing equations for momentum and energy were converted to non-dimensional form and solved using a finite difference scheme that was implemented in C++. The analysis investigated the influence of nanoparticle size ($0.0<\varphi<0.5$) on the thermophysical and Eckert number of 1.0., 20.0, and 40.0 on heat characteristics of the Alumina nanolubricant while maintaining a Reynolds number of 100. The results of the investigation indicate that the thermal conductivity and heat transfer performance of the lubricant are greatly improved by increasing the concentration of $Al_2 O_3$ nanoparticles. The results indicated that maintaining an ideal concentration of nanoparticles leads to a significant enhancement in heat transfer efficiency while minimizing the rise in pressure drop. These results indicate that accurate regulation of nanoparticle concentration is crucial for maximizing the performance of nano-lubricants in heat exchangers, refrigeration systems, and other thermal management systems. This work enhances our knowledge of the appropriate utilization of nanoparticle-enhanced lubricants in industrial processes that need efficient heat dissipation technologies.

Keywords: Nanolubricants, Aluminum Oxide ($Al_2 O_3$), thermophysical properties, heat transfer, flow dynamics, cylindrical channel.

I INTRODUCTION:

Nanotechnology has transformed the field of heat transfer fluids, resulting in the development of nano-lubricants with superior thermophysical properties (Wang & Mujumdar, 2007). Aluminum oxide ($Al_2 O_3$) nano-lubricants have gained popularity due to their high thermal conductivity, chemical stability, and inexpensive cost (Sundar & Sharma, 2010). The concentration of nanoparticles in $Al_2 O_3$ nano-lubricants significantly impacts their thermophysical characteristics and heat transmission performance (Khanafer & Vafai, 2011). Numerical studies indicate that adding $Al_2 O_3$ nanoparticles to base fluids can greatly improve heat transfer rates (Khaleduzzaman & Sohel Murshed, 2015). Further research is needed to optimize the performance of $Al_2 O_3$ nano-lubricants due to their complicated interactions with nanoparticles, base fluid, and channel shape (Yang & Liu, 2018).

International Journal of Advances in Engineering and Management (IJAEM)
Volume 6, Issue 09 Sep. 2024, pp: 499-508 www.ijaem.net ISSN: 2395-5252

Several heat transfer strategies have been developed at a rapid pace in response to the heightened demands for heat transfer enhancement in industrial applications. Nanofluids are employed as efficient working media in heat pipes (Sun et al., 2018), heat exchangers, automobile radiators (Hussein et al., 2014; Selvam et al., 2017), solar energy systems (Chen et al., 2019; Amirahmad et al., 2021), and electronic chips due to their exceptional thermal performance, uniformity, and dispersion stability. Choi was the first to introduce the concept of nanofluid (Carmichael et al., 1963). Nanofluids are stable colloidal suspensions that are produced by dispersing nanoparticles in water, oil, ethylene glycol, and other base fluids. The thermal properties of base fluids, including viscosity and thermal conductivity, are substantially influenced by nanoparticles. Yang et al. (2021), Kumar et al. (2015a), and Sarviya and Fuskele (2017) summarized the theoretical models of the thermal conductivity of nanofluids. The thermal conductivity of nanofluids was determined by these researchers to be primarily influenced by concentration, temperature, nanoparticle diameter, and particle morphology.

The thermal conductivity of the magnesia–ethylene glycol nanofluid increases as the concentration increases within the temperature range of 25 to 100°C. Kumar et al. (2016) demonstrated that the thermal conductivity of 1.25 vol% multiwalled carbon nanotube nanofluids was 122.67% greater than that of water at 35°C. Wang et al. (2021a) discovered that the viscosity of Fe_3O_4–CNT magnetic fluids was 144.2 and 149.9% higher than that of deionized water at concentrations of 0.5 and 1%, respectively. The viscosity of 0.3 wt% MgO–ethylene glycol nanofluids at 25°C increased by 13.8% in the study conducted by Arya et al. (2019). In comparison to water, the viscosities of TiO_2, Al_2O_3, ZnO, and CeO_2 nanofluids were higher than those of the base fluid, and the viscosity of Al_2O_3 nanofluids with a 0.5% volume fraction increased by 10%. This was discovered by Kumar et al. (2016).

The heat transfer efficacy of nanofluids can be improved by various heat transfer mechanisms, particularly for conductive and convective heat transfer (natural convection and forced convection) (Vajjha and Das, 2012; Leela Vinodhan et al., 2016; Yang et al., 2021). Electronic device cooling, solar energy harvesting, energy conversion, food processing, and petrochemical engineering are all applications that extensively employ natural convection, which is induced by temperature differences within a cavity. In a rectangular cavity with a porous medium, Hdhiri et al. (2019) investigated the natural convection of an electrically conductive fluid. They believed that the Prandtl number was a significant factor in determining the average Nusselt number. Souayeh et al. (2020) conducted a three-dimensional numerical analysis of the natural convection heat transfer between the square cavity and the interior sphere in the presence of air. The results indicated that the heat transfer efficacy of the spherical interior was superior to that of the cylindrical interior.

Numerous researchers have investigated the natural convection of nanofluids from a variety of perspectives. In a cavity, Rostami et al. (2020) implemented natural convection by incorporating a variety of nanofluids. The heat transmission characteristics were significantly influenced by the types and concentrations of nanofluids, the shapes of cavities, and the Rayleigh number. They concluded that the heat transmission characteristics in the cavity were compromised as a result of the increase in fluid viscosity caused by nanoparticles. The fluid flow and heat transmission of nanofluids within the cavity were also significantly influenced by the locations of heat sources (Öztop et al., 2015). They determined that there is insufficient generalization between the thermal conditions of the nanofluids in the cavity and their heat transfer characteristics. Electric heating is a practical implementation of natural convective heat transfer in industrial production and daily life.

The objective of this study is to numerically analyze how nanoparticle concentration affects the thermophysical characteristics and heat transfer characteristics of $Al_2\ O_3$ nano-lubricants in a cylindrical channel. The simulation findings will provide useful information about the appropriate nanoparticle concentration for improved heat transmission and thermophysical characteristics. Specifically, this study examined the impact of nanoparticle concentration on thermal conductivity, viscosity, specific heat capacity, and heat transfer characteristics. The results of this study will enhance the advancement of effective heat transfer systems foundation on $Al_2\ O_3$ nano-lubricants for diverse industrial uses.

II. MATERIALS AND METHODS

A. Numerical Model

Figure 1 shows the two-dimensional laminar boundary layer flow of an incompressible Newtonian fluid with viscous fluid on the cylinder's surface. The surface temperature is greater than the

International Journal of Advances in Engineering and Management (IJAEM)
Volume 6, Issue 09 Sep. 2024, pp: 499-508 www.ijaem.net ISSN: 2395-5252

free stream temperature and water contains copper nanoparticles. Laminar natural convection heat transport was simulated in a saturated H_2O-Cu nanofluid vertical cylinder. Free circulation and fluid motion relative to the solid surface come from density change-induced buoyancy and the momentum field accounts for buoyancy forces as body forces. These conditions link continuity, momentum, and energy equations. The thermophysical properties stated in Table 1 are considered to be constant. (Öztop, et al . 2015)

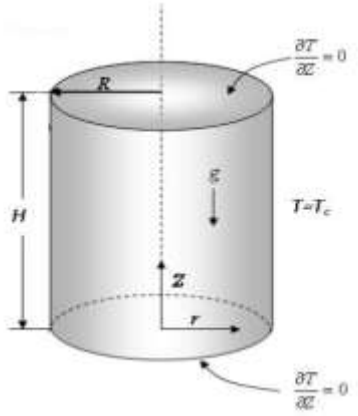

Figure 1: Geometrical configuration, boundary conditions, and coordinate system

B. Governing Equations

The governing mathematical equations were resolved under the following conditions: fluid incompressibility, laminar flow, no internal heat inputs, two-dimensional flow, the Boussinesq approximation, and thermal equilibrium between water and nanoparticles. The current model proposes a laminar, incompressible, viscous-free flow that is constant and two-dimensional. Gravity acts vertically downward, but radiation is disregarded. Mass and momentum conservation formulae are flow-regulating formulae over the continuum (Shahi et al. 2011; Lan and Violi, 2010). The continuity formula is expressed in Eq. (1)

$$\frac{\partial \rho}{\partial t}+\frac{1}{r}\frac{\partial(\rho r v_r)}{\partial r}+\frac{1}{r}\frac{\partial(\rho v_\theta)}{\partial \theta}+\frac{\partial(\rho v_z)}{\partial z}=0 . \quad \textbf{(1)}$$

R and Z Navier-Stokes equations are Eq. (2) and Eq. (3).

$$\rho\left(\frac{\partial v_r}{\partial t}+v_r\frac{\partial v_r}{\partial r}+\frac{v_\theta}{r}\frac{\partial v_r}{\partial \theta}+v_z\frac{\partial v_r}{\partial z}-\frac{v_\theta^2}{r}\right) = -\frac{\partial p}{\partial r}+\mu\left[\frac{\partial}{\partial r}\left(\frac{1}{r}\frac{\partial}{\partial r}(r v_r)\right)+\frac{1}{r^2}\frac{\partial^2 v_r}{\partial \theta^2}+\frac{\partial^2 v_r}{\partial z^2}-\frac{2}{r}\frac{\partial v_\theta}{\partial \theta}\right]+\rho g_r \quad (2)$$

$$\rho\left(\frac{\partial v_z}{\partial t}+v_r\frac{\partial v_z}{\partial r}+\frac{v_\theta}{r}\frac{\partial v_z}{\partial \theta}+v_z\frac{\partial v_z}{\partial z}\right) = -\frac{\partial p}{\partial z}+\mu\left[\frac{1}{r}\frac{\partial}{\partial r}\left(r\frac{\partial v_z}{\partial r}\right)+\frac{1}{r^2}\frac{\partial^2 v_z}{\partial \theta^2}+\frac{\partial^2 v_z}{\partial z^2}\right]+\rho g_z \quad (3)$$

Equation (4) provides the formula for thermal energy exchange

$$\rho_{nf}\left(c_p\right)_{nf}\left(u\frac{\partial T}{\partial r}+v\frac{\partial T}{\partial z}\right)=k_{nf}\left(\frac{\partial^2 T}{\partial r^2}+v\frac{\partial^2 T}{\partial z^2}\right). \quad \textbf{(4)}$$

The nanofluid heat capacity $\left(c_p\right)_{nf}$, density, ρ_{nf}, thermal expansion coefficient, β_{nf}, and thermal diffusivity, α_{nf} are expressed in Eq. (5-11), (Salah et al. 2011; Nazar, et al. 2011; Esmaeilpour and Abdollahzadeh, 2012)

Equation (5) provides an approximation of the nanofluid's effective thermal conductivity

$$\frac{k_{nf}}{k_f}=\frac{k_{au}+2k_f-2\varphi\left(k_f-k_{au}\right)}{k_{au}+2k_f+\varphi\left(k_f-k_{au}\right)} \quad (5)$$

Table 1: Water-Al_2O_3 Nanofluid's Thermophysical Characteristics

	Density (kgm^{-3})	Heat Capacity ($J/kg^{-1}K^{-1}$)	Thermal Conductivity ($Wm^{-1}K^{-1}$)	Thermal expansion (K^{-1})	Viscosity
H_2O	997.1	4179	0.613	$21x10^{-5}$	$9.09x10^{-5}$
Al_2O_3	3880	773	36	$2.43x10^{-5}$	2.0

This equation only applies to spherical nanoparticles and does not address other nanoparticle shapes. This model is appropriate for studying nanofluid-enhanced heat transfer [7–10]. Eq.(6) provides the viscosity of the nanofluid. (Esmaeilpour and Abdollahzadeh, 2012)

$$\mu_{nf}=\mu_f\left(1-\varphi\right)^{-2.5} \quad (6)$$

Equation (7) is the formula for the nanofluid's density [10]

$$\rho_{nf}=\left(1-\varphi\right)\rho_f+\varphi\rho_{au} \quad (7)$$

Equation (8) expresses the nanofluid's heat capacitance (Nazar, et al. 2011; Esmaeilpour and Abdollahzadeh, 2012)

$$\left(\rho c_p\right)_{nf}=\left(1-\varphi\right)\left(\rho c_p\right)_f+\varphi\left(\rho c_p\right)_{au} \quad (8)$$

The nanofluid's thermal expansion coefficient is written in Eq (9) (Esmaeilpour and Abdollahzadeh, 2012):

International Journal of Advances in Engineering and Management (IJAEM)
Volume 6, Issue 09 Sep. 2024, pp: 499-508 www.ijaem.net ISSN: 2395-5252

$$(\rho\beta)_{nf} = (1-\varphi)(\rho\beta)_f + \varphi(\rho\beta)_{au} \quad (9)$$

Eq. (10) provides the nanofluid's thermal diffusivity (Esmaeilpour and Abdollahzadeh, 2012):

$$\alpha_{nf} = \frac{k_{nf}}{(\rho c_p)_{nf}} \quad (10)$$

C. Analytical Techniques and Solution Schemes

Hyperbolic, elliptic, or parabolic Partial derivative formulae are Navier-Stokes equations. The pressure gradient between equations (2) and (3) was eliminated using the vorticity-stream technique. Equation (11) illustrates the vortex scattering transport expression by employing the continuity concept from equation (1).

$$\omega = \frac{\partial v}{\partial r} - \frac{\partial u}{\partial z} \quad \textbf{(11)}$$

The dimensional vorticity transmission equation is given in equation (12)

$$u\frac{\partial \omega}{\partial r} + v\frac{\partial \omega}{\partial z} = -\beta g\frac{\partial T}{\partial r} + \upsilon\left(\frac{\partial^2 \omega}{\partial r^2} + \frac{\partial^2 \omega}{\partial z^2}\right) \quad (12)$$

Equation (13) utilizes stream function derivatives to define velocity in two-dimensional cylindrical dimensions.

$$u = \frac{\partial \psi}{\partial z}, \quad v = -\frac{\partial \psi}{\partial r} \quad (13)$$

Equation (14) offers the Poisson formula when substituted in Eq.(11)

$$\omega = -\left(\frac{\partial^2 \psi}{\partial r^2} + \frac{\partial^2 \psi}{\partial z^2}\right) \quad (14)$$

The transport equation, energy equation, and operational conditions were converted to a non-dimensional notation for a variety of physical parameters, using L, U_W, (T_w - T_∞), $\psi_W L$, and ω_W / L respectively for length, velocity, temperature, stream function, and vorticity as shown in Eq.(15), (Sangotayo and Hunge, 2020).

$$Z = \frac{z}{L}, \quad R = \frac{r}{L}, \; V = \frac{v}{U_w}, \quad U = \frac{u}{U_w},$$

$$\theta = \frac{(T - T_\infty)}{(T_w - T_\infty)}, \; \Omega = \frac{\omega}{U_w / L}, \quad \Psi = \frac{\psi}{U_w L}, \quad (15)$$

Eq. (16–19) provides the normalized equations for the R- and Z-velocity components, vortex shedding, stream constituent, and energy transport:

$$U = \frac{\partial \varphi}{\partial Z}, \quad V = -\frac{\partial \varphi}{\partial R} \quad (16)$$

$$\omega = -\frac{\partial^2 \varphi}{\partial Z^2} - \frac{\partial^2 \varphi}{\partial R^2} \quad (17)$$

$$U\frac{\partial \omega}{\partial Z} - V\frac{\partial \omega}{\partial R} = Ra\,\mathrm{Pr}\frac{\beta_{nf}}{\beta_f}\frac{\partial \theta}{\partial Z} + \frac{\mu_{nf}}{\rho_{nf}\alpha_{nf}}\left(\frac{\partial^2 \omega}{\partial Z^2} + \frac{\partial^2 \omega}{\partial Z^2}\right)$$

(18)

$$U\frac{\partial \theta}{\partial Z} - V\frac{\partial \theta}{\partial R} = \frac{\alpha_{nf}}{\alpha_f}\left(\frac{\partial^2 \theta}{\partial Z^2} + \frac{\partial^2 \theta}{\partial Z^2}\right) \quad (19)$$

Where μ is dynamic viscosity, k is thermal conductivity, Ra is Rayleigh number, Gr is Grashof number, Re is Reynolds number, Pr is Prandtl number and Cp is specific heat capacity,
Non-dimensional border conditions are:

$\Omega \neq 0;\ V = 0;\ \Psi \neq 0;\ \theta = U = 1$ at $Z = 1;\ 0 \leq R \leq 1$;

$U = \Psi = \theta = V = 0;\ \Omega \neq 0;\ at\ Z = 0;\ 0 \leq R \leq 1;$

$V = \theta = U = \Psi = 0;\ \Omega \neq 0\ at\ R = 0;\ 0 \leq Z \leq 1;$

$\Psi = \frac{\partial U}{\partial R} = \frac{\partial \theta}{\partial R} = \frac{\partial V}{\partial R} = 0;\ \Omega \neq 0$ at $R = 1;\ 0 \leq Z \leq 1$.

One of the most effective problem-solving techniques for nonlinear energy transport and vorticity formulae (18) and (19) is the finite difference approach. The concurrent system of equations was assessed by utilizing heat transmission and relaxation between a fluid and a surface, which resulted in a temperature gradient that was proportional to the neighboring Nusselt quantity, as illustrated in Eq. (20). (Waheed, 2009).

$$Nu_x = \frac{hr}{k} = -\left(\frac{\partial \theta}{\partial Z}\right)_{Z=1} \quad (20)$$

Eq. (20) is the enclosed Nusselt number across the heated contact space yields the usual Nusselt quantity as shown in Eq. (21) (Waheed, 2009).

$$N\bar{u} = \frac{\dot{Q}_{conv}}{\dot{Q}_{cond}} = -\int_0^1 \left.\frac{\partial \theta}{\partial Z}\right|_{Z=0\,or\,1} dR \quad (21)$$

The Rayleigh number (Ranf) of the nanofluid was determined using Equation (22) and the Grashof number (Grnf) was determined using Equation (23). The Buoyancy factor (BFnf) was determined using Equation (24). (Esmaeilpour and Abdollahzadeh, 2012; Waheed, 2009).

$$Ra_{nf} = \frac{g\beta_{nf} H^3}{\alpha_{nf}\mu_{nf}} \quad (22)$$

$$Gr_{nf} = \frac{Ra_{nf}}{\mathrm{Pr}_{nf}} \quad (23)$$

$$BF_{nf} = \frac{Gr_{nf}}{\sqrt[3]{\mathrm{Re}}} \quad (24)$$

International Journal of Advances in Engineering and Management (IJAEM)
Volume 6, Issue 09 Sep. 2024, pp: 499-508 www.ijaem.net ISSN: 2395-5252

The temperature and vortex fields were established in accordance with the conditions for stable flow, as illustrated in Eq. (25): (Sangotayo and Hunge, 2020)

$$\frac{\sum_{i=2}^{N}\sum_{j=2}^{M}\left|\phi_{ij}^{n+1}-\phi_{ij}^{n}\right|}{\sum_{i=2}^{N}\sum_{j=2}^{M}\left|\phi_{ij}^{n+1}\right|}<\delta \qquad (25)$$

The variable ϕ denotes Ω, Ψ or θ, and n refer to the number of iterations required for convergence of the outcomes. The value utilized varies between 10^{-3} and 10^{-8} in distinct forms of literature (Sangotayo and Hunge, 2020)

III RESULTS AND DISCUSSIONS

Figure 2 shows the results of estimating the local Nusselt number at different convergence factor values (ranging from 10^{-1} to 10^{-8}), to evaluate the effect of the convergence standard on numerical results. According to Sangotayo and Hunge (2020), grid independence studies reveal that a 41 by 41 grid layout is sufficient for excellent numerical solutions, field precision, and high accuracy. The results imply a convergence factor of 10^{-4}.

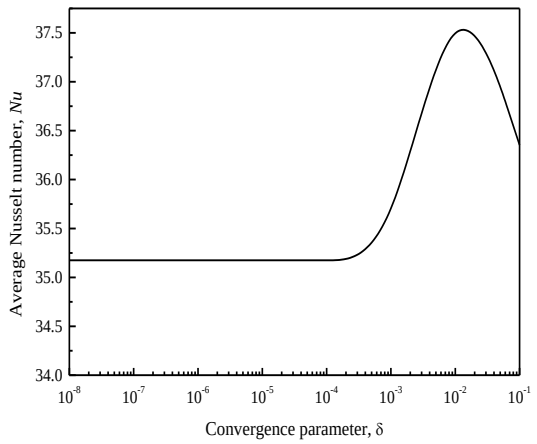

Fig. 2. A graph of the mean Nusselt number, Nu, versus convergence variable. δ

Fig. 3 shows how changing the nanoparticle sizes and the Eckert number between 1 and 40 affects the Nusselt number. The Nusselt values increase with the increase in Eckert values. As Ec increases, the Nusselt number (Nu) increases, which suggests that the heat transfer process is more efficient. Additionally, the convective heat transfer coefficient and the temperature gradient near the wall increase. The Nusselt number (Nu) increases as the size of the nanoparticles decreases from 0.5 to 0.0, which suggests that heat transfer is improved. Additionally, the convective heat transfer coefficient increases and the thickness of the thermal boundary layer diminishes. Comprehending the impact of nanoparticle size and Ec on Nu is essential for the design of effective heat transfer systems.

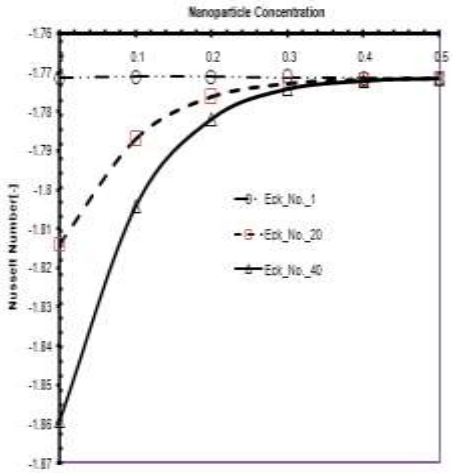

Fig. 3 The influence of altering the nanoparticle sizes and Eckert number on the Nusselt number

Figure 3 shows how adjusting the nanoparticle sizes between 0 and 0.5 affects the Prandtl number Prandtl values fall as nanoparticle size increases to 0.3 and this suggests that while heat diffusivity is increasing, momentum diffusivity is rapidly decreasing.

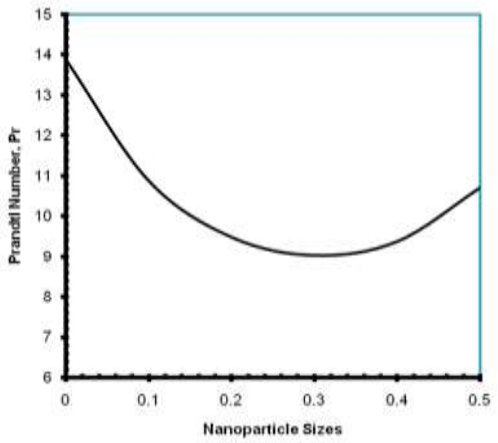

Fig. 4 The influence of altering the nanoparticle sizes on the Prandtl number

International Journal of Advances in Engineering and Management (IJAEM)
Volume 6, Issue 09 Sep. 2024, pp: 499-508 www.ijaem.net ISSN: 2395-5252

Fig. 5 displays the influence of altering nanoparticle fraction on the local drag coefficient. It shows that the local drag coefficient reduces as nanoparticle fraction increases. The local drag coefficient diminishes with an increase in nanoparticle percentage due to enhanced viscosity; nanoparticles elevate the viscosity of the base fluid, hence decreasing turbulence and drag. Furthermore, nanoparticles augment the boundary layer thickness, hence diminishing velocity gradients and drag. It is supported by Hwang et al. (2016) and Pouranfard et al. (2014)

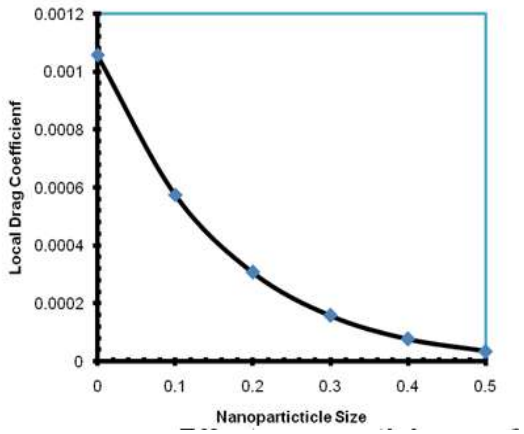

Fig. 4 The influence of altering nanoparticle fraction on Local Drag Coefficient

Figure 5 illustrates the impact of modifying nanoparticle sizes ranging from 0 to 0.5 on the density of the nanofluid. As the size of nanoparticles grows, the density of the nanofluid rises due to a greater mass fraction of nanoparticles and enhanced nanoparticle aggregation, resulting in a bigger effective particle size. It was collaborated by Wang et al. (2006).

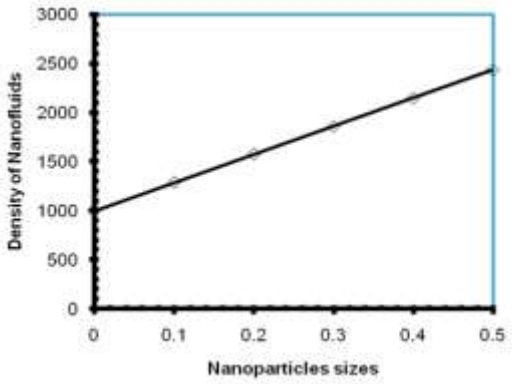

Fig. 5 **Effect of nanoparticle sizes on the density of nanofluids**

Figure 6 illustrates the impact of modifying nanoparticle sizes ranging from 0 to 0.5 on the viscosity of the nanofluid. The viscosity of nanofluids increases as the size of the nanoparticles increases, which is a result of the increased surface area. The interactions with the base fluid are enhanced by the larger nanoparticles' higher surface area-to-volume ratio. Clusters are formed by larger nanoparticles, which aggregate and increase viscosity. The viscosity of the base fluid is increased by the fact that larger nanoparticles interact with it more strongly.

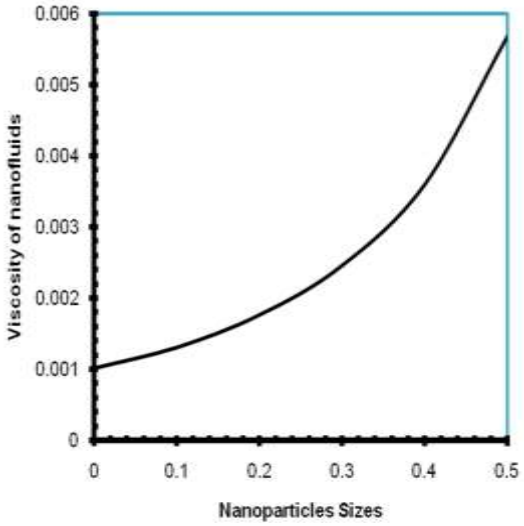

Fig. 6 **Effect of nanoparticle sizes on the viscosity of nanofluids**

Figure 7 illustrates the effect of adjusting the size of nanoparticles from 0 to 0.5 on the thermal conductivity of the nanofluid. The thermal conductivity of nanofluids increases as the size of nanoparticles increases because of their increased surface area. The surface area-to-volume ratio of larger nanoparticles is higher, improving heat transfer and Clusters of larger nanoparticles increase heat conductivity. Larger nanoparticles show enhanced Brownian motion and promote phonon transport, both of which boost thermal conductivity.

International Journal of Advances in Engineering and Management (IJAEM)
Volume 6, Issue 09 Sep. 2024, pp: 499-508 www.ijaem.net ISSN: 2395-5252

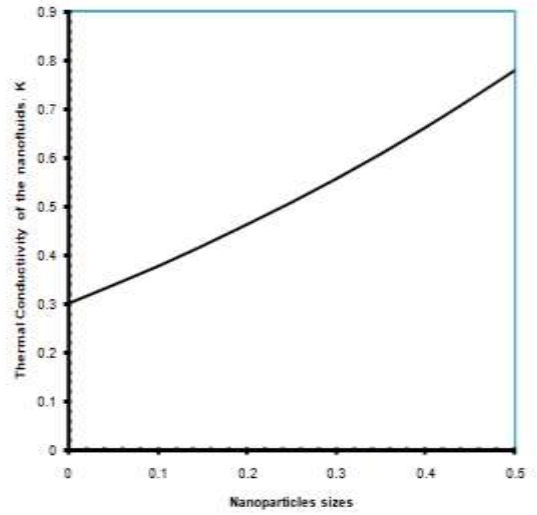

Fig. 7 Effect of nanoparticle sizes on the thermal conductivity of nanofluids

The effect of adjusting nanoparticle sizes between 0 and 0.5 on the nanofluid's specific heat capacity is shown in Figure 8. The specific heat capacity of nanofluids decreases as the size of nanoparticles increases because larger nanoparticles have a lower surface area and display diminished Brownian motion, which limits heat transmission, they have a lower specific heat capacity than smaller nanoparticles in nanofluids. Larger nanoparticles tend to agglomerate more, which lowers their specific heat capacity and effective surface area.

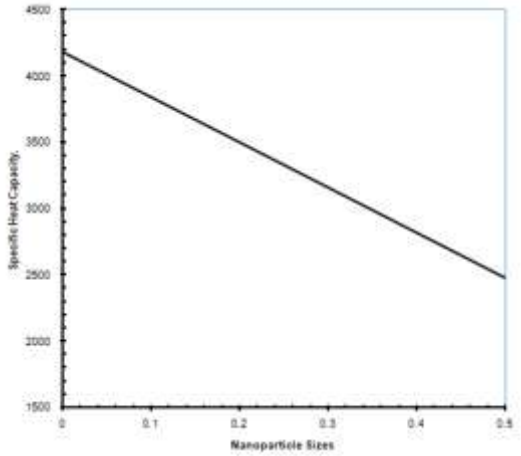

Fig. 8 Effect of nanoparticle sizes on the specific heat capacity of nanofluids

Fig. 9 shows how changing the nanoparticle sizes and the Eckert number between 1 and 40 affects the heat characteristics of nanofluids. Heat characteristics, including thermal conductivity and heat transfer coefficient, increase with nanoparticle size and decrease with Eckert number. This is because larger nanoparticles have a higher surface area-to-volume ratio, which increases thermal conductivity. Enhanced particle-fluid interactions and the thickness of the thermal boundary layer are reduced by larger nanoparticles, which in turn improves heat transfer. Eckert Number is the ratio of kinetic energy to thermal energy is denoted by Ec. An increase in Ec results in a reduction in heat transfer as a result of the increased thickness of the thermal boundary layer.

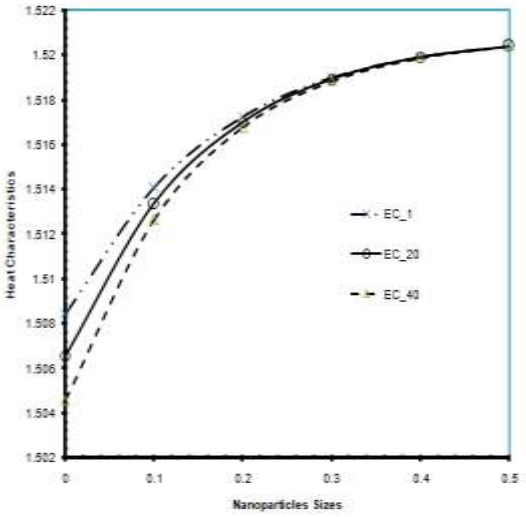

Fig. 9 Effect of nanoparticle sizes and Eckert number on Heat characteristics of nanofluids

The analysis indicates that there is a perfect amount of nanoparticles that increases heat transfer efficiency while reducing adverse consequences, such as increased pressure drop. This balance is crucial for ensuring that the nano-lubricant improves thermal efficiency without incurring excessive operational costs or inefficiencies. The research emphasizes the importance of accurately adjusting the proportion of nanoparticles in nano-lubricants to enhance heat dissipation in industrial processes, including thermal systems, refrigeration systems, and heat exchangers.

IV CONCLUSIONS

This study provided a thorough numerical analysis of the impact of nanoparticle concentration on the thermophysical properties and heat transfer performance of aluminum oxide ($Al_2 O_3$)-based nano-lubricants in a cylindrical channel. The findings indicated that the thermal conductivity and

heat transfer capabilities of the nano-lubricant are considerably improved by the increase in the concentration of $Al_2 O_3$ nanoparticles. The thermal conductivity, viscosity, and density of the $Al_2 O_3$ nanofluid increases as the size of the nanoparticles increases. As the nanoparticle fraction increases, the local drag coefficient and specific thermal capacity of the nanofluid decreases. Heat characteristics, such as thermal conductivity and heat transfer coefficient, increase with nanoparticle size and diminish with Eckert number. The results provide valuable insights into the design and application of nanoparticle-enhanced lubricants for thermal management and emphasize the potential of $Al_2 O_3$ nano-lubricants to enhance heat transfer performance in a diverse array of engineering applications, provided that the concentration of nanoparticles is meticulously managed. To enhance the efficacy of nano-lubricants, future research could investigate the impact of various nanoparticle materials, base fluids, and flow conditions.

REFERENCES

[1]. Amirahmad, A., Maglad, A. M., Mustafa, J., and Cheraghian, G. (2021). Loading PCM into Buildings Envelope to Decrease Heat Gain-Performing Transient Thermal Analysis on Nanofluid Filled Solar System. Front. Energ. Res. 9, 727011.doi:10.3389/fenrg.2021.727011

[2]. Arya, H., Sarafraz, M. M., Pourmehran, O., and Arjomandi, M. (2019). Heat Transfer and Pressure Drop Characteristics of MgO Nanofluid in a Double Pipe Heat Exchanger. Heat Mass. Transfer 55, 1769–1781. doi:10.1007/s00231-018-02554-1

[3]. Carmichael, L. T., Berry, V., and Sage, B. H. (1963). Thermal Conductivity of Fluids. Ethane. J. Chem. Eng. Data 8, 281–285. doi:10.1021/je60018a001

[4]. Chen, W., Zou, C., and Li, X. (2019). Application of Large-Scale Prepared MWCNTs Nanofluids in Solar Energy System as Volumetric Solar Absorber. Solar Energy. Mater. Solar Cell 200, 109931. doi:10.1016/j.solmat.2019.109931

[5]. Esmaeilpour, M. and Abdollahzadeh, M. (2012) "Free convection and entropy generation of nanofluid inside an enclosure with different patterns of vertical wavy walls", International Journal of Thermal Science, vol. 52, pp. 127-136

[6]. Hdhiri, N., Souayeh, B., Alfannakh, H., and Beya, B. B. (2019). Natural Convection Study with Internal Heat Generation on Heat Transfer and Fluid Flow within a Differentially Heated Square Cavity Filled with Different Working Fluids and Porous Media. BioNanoSci. 9, 702–722. doi:10.1007/s12668-019-00626-y

[7]. Hussein, A. M., Bakar, R. A., and Kadirgama, K. (2014). Study of Forced Convection Nanofluid Heat Transfer in the Automotive Cooling System. Case Stud. Therm. Eng. 2, 50–61. doi:10.1016/j.csite.2013.12.001

[8]. Hwang et al. (2016). Experimental investigation of drag reduction in nanofluids. Journal of Mechanical Science and Technology, 30(5), 2261-2268.

[9]. Khaleduzzaman, S. S., & Sohel Murshed, S. M. (2015). Numerical investigation of heat transfer enhancement using alumina-water nanofluid in a circular pipe. International Journal of Heat and Mass Transfer, 81, 415-424.

[10]. Khanafer, K., & Vafai, K. (2011). A critical synthesis of thermophysical characteristics of nanofluids. International Journal of Heat and Mass Transfer, 54(19-20), 4410-4428.

[11]. Kumar, P. M., Kumar, J., Tamilarasan, R., Sendhilnathan, S., and Suresh, S. (2015). Review on Nanofluids Theoretical Thermal Conductivity Models. Ej 19, 67–83. doi:10.4186/ej.2015.19.1.67

[12]. Kumar, V., Tiwari, A. K., and Ghosh, S. K. (2016). Effect of Variable Spacing on Performance of Plate Heat Exchanger Using Nanofluids. Energy 114, 1107–1119. doi:10.1016/j.energy.2016.08.091

[13]. Leela Vinodhan, V., Suganthi, K. S., and Rajan, K. S. (2016). Convective Heat Transfer Performance of CuO-Water Nanofluids in U-Shaped Minitube: Potential for Improved Energy Recovery. Energ. Convers. Management 118, 415–425. doi:10.1016/j.enconman.2016.04.017

[14]. Lin, K.C. and Violi, A. (2010) "Natural convection heat transfer of nanofluids in a vertical cavity: Effects of nonuniform particle diameter and temperature on thermal conductivity", International Journal of Heat and Fluid Flow, vol. 31, pp. 236-245

[15]. Nazar, R. Tham, L. Pop, I. and Ingham, D.B. (2011) "Mixed convection boundary layer flow from a horizontal circular cylinder embedded in a porous medium filled with a nanofluid", Transport in Porous Media. 86(2), pp. 517-536

[16]. Öztop, H. F., Estellé, P., Yan, W.-M., Al-Salem, K., Orfi, J., and Mahian, O. (2015). A Brief Review of Natural Convection in Enclosures under Localized Heating with and without Nanofluids. Int. Commun. Heat Mass Transfer 60, 37–44. doi:10.1016/j.icheatmasstransfer.2014.11.001

[17]. Pouranfard, Abdolrasoul & Mowla, D. & Esmaeilzadeh, Feridun. (2014). An experimental study of drag reduction by nanofluids through horizontal pipe turbulent flow of a Newtonian liquid. Journal of Industrial and Engineering Chemistry. 20. 633–637. 10.1016/j.jiec.2013.05.026.

[18]. Rostami, S., Aghakhani, S., Hajatzadeh Pordanjani, A., Afrand, M., Cheraghian, G., Oztop, H. F., et al. (2020). A Review of the Control Parameters of Natural Convection in Different Shaped Cavities with and without Nanofluid. Processes 8, 1011. doi:10.3390/pr8091011

[19]. Saleh, H. Roslan, R. and Hashim, I. (2011) "Natural convection heat transfer in a nanofluid filled trapezoidal enclosure", International Journal of Heat and Mass Transfer, vol. 54, pp. 194-201

[20]. Sangotayo E. O. and Hunge O. N., (2020) " Numerical Analysis of Nanoparticle Concentration Effect on Thermo-physical Properties of Nanofluid in a Square Cavity " , International Journal of Mechanical and Production Engineering, vol. 8, no. 2, pp. 18-23,

[21]. Sarviya, R. M., and Fuskele, V. (2017). Review on thermal Conductivity of Nanofluids. Mater. Today Proc. 4, 4022–4031. doi:10.1016/j.matpr.2017.02.304

[22]. Selvam, C., Mohan Lal, D., and Harish, S. (2017). Enhanced Heat Transfer Performance of an Automobile Radiator with Graphene-Based Suspensions. Appl. Therm. Eng. 123, 50–60. doi:10.1016/j.applthermaleng.2017.05.076

[23]. Shahi, M. Mahmoudi, A.H. and Talebi, F. (2011) "A numerical investigation of conjugated-natural convection heat transfer enhancement of a nanofluid in an annular tube driven by inner heat generating solid cylinder", International Communication of Heat and Mass Transfer, vol. 38, no. 4, pp. 533-542

[24]. Souayeh, B., Hdhiri, N., Alam, M. W., Hammami, F., and Alfannakh, H. (2020). Convective Heat Transfer and Entropy Generation Around a Sphere within Cuboidal Enclosure. J. Thermophys. Heat Transfer 34, 605–625. doi:10.2514/1.T5960

[25]. Sun, B., Peng, C., Yang, D., and Li, H. (2018). Effect of the Wick and the Working Medium on the Thermal Resistance of FPHP. Front. Energ. Res. 6, 37. doi:10.3389/fenrg.2018.00037

[26]. Sundar, L. S., & Sharma, K. V. (2010). Thermal conductivity of nanofluids. International Journal of Nanoparticles, 3(1), 21-38.

[27]. Vajjha, R. S., and Das, D. K. (2012). A Review and Analysis of the Influence of Temperature and Concentration of Nanofluids on Thermophysical Properties, Heat Transfer and Pumping Power. Int. J. Heat Mass Transfer 55, 4063–4078. doi:10.1016/j.ijheatmasstransfer.2012.03.048

[28]. Waheed, M. A. (2009) "Mixed convective heat transfer in rectangular enclosures driven by a continuously moving horizontal plate", International Journal of Heat and Mass Transfer, vol. 52, pp. 5055–5063

[29]. Wang j., Li, G., Li, T.,. (2006). Thermal conductivity and density of nanofluids. Journal of Thermophysics and Heat Transfer, 20(4), 847-853.

[30]. Wang, J., Li, G., Li, T., Zeng, M., and Sundén, B. (2021). Effect of Various Surfactants on Stability and Thermophysical Properties of Nanofluids. J. Therm. Anal. Calorim. 143, 4057–4070. doi:10.1007/s10973-020-09381-9

[31]. Wang, X., & Mujumdar, A. S. (2007). Heat transfer characteristics of nanofluids: A review. International Journal of Thermal Sciences, 46(1), 1-19.

[32]. Yang, T., Zhao, P., Li, Q., Zhao, Y., and Yu, T. (2021). Study on Thermophysical Properties of a lead-bismuth-based Graphene Nanofluid. Front. Energ. Res. 9, 727447. doi:10.3389/fenrg.2021.727447

[33]. Yang, Y., & Liu, G. (2018). Numerical study on heat transfer enhancement of

$Al_2 O_3$ -water nanofluid in a cylindrical heat exchanger. Applied Thermal Engineering, 129, 1451-1460.

NOMENCLATURE

Symbols	Definitions	Unit
m	Mass flow rate	[kg/hr]
Qu	Useful energy	[W]
C_p	Heat capacity	[J/kg.K]
Cp_{nf}	Nanofluid heat capacity	[J/kg.K]
Cp_f	Fluid heat capacity	[J/kg.K]
Cp_p	Nanoparticle heat capacity	[J/kg.K]
K_f	Fluid thermal conductivity	[W/m.K]
K_p	Nanoparticle thermal conductivity	[W/m.K]
□□□	Nanofluid thermal conductivity	[W/m.K]

Greek Symbols

Symbols	Definitions	Unit
□□□	Nanofluid density	[kg/□^{3}]
□	Nanoparticle size	[-]
□□	Fluid density	[kg/□^{3}]
□□□	Nanofluid viscosity	[m²/s]
□□	Nanoparticle density	[kg/□^{3}]
□□	Fluid viscosity	[m²/s]

Subscripts

nf	Nanofluid
p	Particle
f	Fluid
Bf	Base Fluid

Greek symbols

μ	viscosity
φ	Volume fraction
ρ	Density